UC Irvine
UC Irvine Previously Published Works

Title
Data acquisition card for fluctuation correlation spectroscopy allowing full access to the detected photon sequence

Permalink
https://escholarship.org/uc/item/7wm002c7

Journal
Review of Scientific Instruments, 71(2 I)

ISSN
0034-6748

Authors
Eid, JS
Müller, JD
Gratton, E

Publication Date
2000

DOI
10.1063/1.1150208

Peer reviewed

Data acquisition card for fluctuation correlation spectroscopy allowing full access to the detected photon sequence

John S. Eid,[a)] Joachim D. Müller, and Enrico Gratton
Laboratory for Fluorescence Dynamics, Department of Physics, University of Illinois at Urbana-Champaign, Urbana, Illinois 61801-3080

Typically, fluctuation correlation spectroscopy (FCS) data acquisition cards measure the number of photon events per time interval (i.e., bin)—time mode. Commercial FCS cards combine the bins through hardware in order to calculate the autocorrelation function. Such a design therefore does not yield the time resolved photon sequence, but only the autocorrelation of that sequence. A different acquisition method which measures the number of time intervals between photon events has been implemented—photon mode. This method takes advantage of the fact that in FCS the rate of photon counts is much less than the frequency of the clock that is used to determine the temporal location of the photons. By using this new mode of data acquisition, the current card design allows for 25 ns time resolution. The data acquisition card can operate in both time and photon mode and yields the time resolved sequence of photon arrivals in both cases. Therefore, the data is available for analysis by any method(s), such as but not limited to, autocorrelation, photon counting histogram, and higher order autocorrelation. © *2000 American Institute of Physics.* [S0034-6748(00)05202-3]

I. INTRODUCTION

Fluctuation correlation spectroscopy (FCS) is a technique used to obtain kinetic information through analysis of the stochastic fluctuations in a molecule's fluorescence.[1] FCS obtains kinetic information by calculating the correlation in the emitted photon sequence. For example, since the excitation volume is known, the correlation resulting from the time it takes for a dye to cross this volume intrinsically yields a diffusion coefficient. In addition, any property which causes fluctuations in the fluorescence intensity of the dye at a rate fast enough to occur during the fraction of time when the dye is in the excitation volume, will be captured by the autocorrelation function. Therefore, such processes as rotational diffusion,[2,3] triplet state formation,[4] and chemical reactions[5–9] can all be measured using this technique. For the most part, commercially available hardware correlators are used to perform the autocorrelation in FCS experiments. The electronics of the commercial correlator boards determine the autocorrelation function by a time resolved binning of the photon counts.[10] The width of the time bin determines the temporal resolution of the autocorrelation function.

However, autocorrelation is not the only analysis that one can perform on the stream of photon counts. Since the determination of the autocorrelation function is a data reduction technique, some of the information embedded in the temporal sequence of the detected photons is lost. Other analysis techniques can yield additional information not contained in the autocorrelation. For example, photon counting histogram (PCH) analysis,[11] higher order autocorrelation,[12,13] and moment analysis[14] have been introduced to analyze fluorescence fluctuation data. So any data acquisition method that only determines the autocorrelation, but does not return

the complete time resolved sequence of photon events, neglects useful information. In order to avoid this limitation a data acquisition card which returns the entire time sequence of photon arrivals was developed.

II. CIRCUIT PHILOSOPHY

The card is designed so that it can acquire data in two different modes, which we call time and photon mode. Time mode determines the number of detected photons that occur within a fixed bin size determined by the frequency of the clock. Photon mode, on the other hand, determines the number of clock cycles between successive photon events. A schematic description of these two modes is shown in Fig. 1. In time mode the time lapse between two successive clocks determines the bin and the counts are given by the photon events. In photon mode the bin is determined by two successive photons and the clock yields the counts. In either mode the time resolution of the data is determined by the frequency of the clock. However, the data transfer rate to the host computer is mode dependent. Data is transferred at the frequency of the clock in time mode and at the frequency of the photon counts in photon mode.

If the clock frequency is greater then the average photon rate, then the data transfer efficiency of the photon mode is greater then for the time mode. This difference in the data transfer efficiency between the two modes is crucial because achieving a time resolution of 100 ns or better requires a clock frequency of 10 MHz or faster. Even with current computing speed [e.g., peripheral component interconnect (PCI) architecture], transferring data from a peripheral device through the computer's bus at that frequency over an extended period of time, is not trivial. Commercial autocorrelators get around this problem by transferring the autocorrelation and not the raw data, thus limiting their applicability as

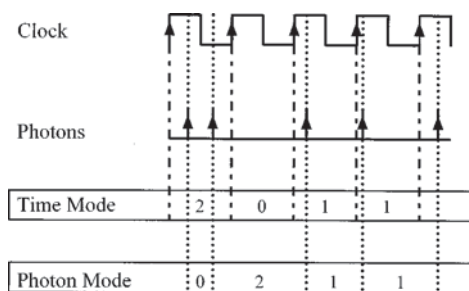a)Electronic mail: johneid@students.uiuc.edu

FIG. 1. Comparison between the two modes of operation of the card. In the time mode the data stored represents the number of photon events occurring between successive rising edges of the clock. In the photon mode the data stored represents the number of rising edges of the clock occurring between successive photon events. The time and photon modes transfer data at a rate that is dictated by the frequency of the clock and the frequency of the photons, respectively. In both modes the time resolution is determined by the clock frequency. For a typical FCS experiment the average photon rate is on the order of 100 000 cps and in order to achieve 100 ns time resolution the clock must be set to 10 MHz. In this example the data transfer rate would be 10 MHz for the time mode and 100 kHz for the photon mode.

mentioned earlier. On the other hand, by using the photon mode one can transfer all of the data at a transfer speed of the incoming photon rate. It is our experience that the photon rate of most FCS experiments is relatively low. Experiments are typically designed, so that on average about one molecule resides in the observation volume. The corresponding photon count rates are thus on the order of 100 000 counts per second (cps) or less. In other words, the photon mode is a data compression method that takes advantage of the fact that the clock frequency used is usually much greater than the average photon rate. We discuss the differences between the two modes, show time and photon mode data, and describe the circuitry of our acquisition card.

III. EXPERIMENTAL SETUP AND PROCEDURES

The overall experimental setup is shown in Fig. 2. A more detailed description is given by Berland et al.[15] The laser used as the two photon excitation source is a mode
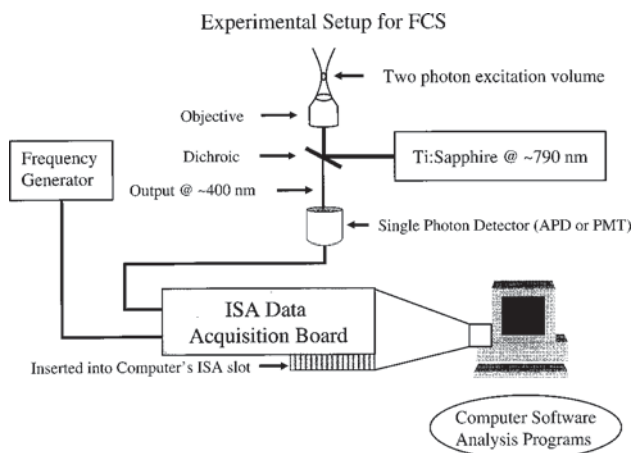

FIG. 2. Experimental setup involving a mode-locked, pulsed, femtosecond Ti:sapphire laser. The two-photon excitation wavelength used was 790 nm and the emission was in the range of 400 nm. The digital acquisition card has two TTL inputs and its output is directly attached to the computer's bus. In initial tests either an additional frequency generator or a double pulse generator was used instead of the output from the photon detector.

locked Ti:sapphire (Mira 900, Coherent, Palo Alto, CA) pumped by an Innova 410 argon ion laser (Coherent, Palo Alto, CA). The detection of emitted photons is through an inverted Zeiss Axiovert 135 TV microscope (Thornwood, NY) with a 63× Fluar oil immersion objective (numerical aperature=1.3). The one channel version of the card is a 16 bit industry standard architecture (ISA) board that has two inputs. The two inputs are the clock and the photon events. The photon events come from either a photomultiplier tube (Hamamatsu, R5600-04-P) or an avalanche photodiode (APD) photon counting unit (EG & G, SPCM-AQ-141). Since the APD unit outputs TTL pulses it is directly hooked up to the card. The photo multiplier tube (PMT) signal on the other hand first goes through an amplifier (Phillips Scientific: Model 6931, Ramsey, NJ) and is then passed through to a discriminator (Phillips Scientific: Model 6930) that outputs TTL pulses. The stored time sequence of photon events was analyzed by programs written for PV-Wave version 6.10 (Visual Numerics, Inc.) and with LFD Globals Unlimited software (Champaign, IL).

Rhodamine purchased from Molecular Probes (Eugene, OR) was dissolved in de-ionized water to a final concentration of approximately 3 nM. Then 500 μL from this dilution was placed on a hanging drop slide with a cover slip placed on top to make a watertight seal with the surface of the slide. The 20 base pair DNA duplex purchased from Midland (Midland, TX) was singly labeled with fluorescein and purified.[16] It was then diluted to a concentration of 30 nM in buffer. The pH 8.4 buffer used consisted of 50 mM TrisCl, 200 mM NaCl, and 0.5 mM ethylenediaminetetraacetic acid. Then 0.8 M urea was added to the DNA-buffer solution. Approximately 500 μL of this sample was placed in one well of an eight chamber cover glass system (Nalge Nunc Inc., Naperville, IL).

IV. OVERALL CIRCUIT SETUP

The main design goal was to create a data acquisition board that preserved the entire time sequence of photon arrivals at a resolution of 100 ns or better. The detected photon sequence would then be transferred to computer memory and analyzed by software at some later point.

The overall structure of the data acquisition card can be seen in Fig. 3. There are four major components to the circuit. The first is the control logic that allows for switching between the two modes of the circuit as well as initialization of the card. The second component is the pulse generating logic. Two pulses are created causing a read of the counters' output by the first in, first outs (FIFOs) followed by a reset of the counters. The third major component of the circuit consists of the four four bit counters which are incremented by the rising edge of the event signal during the temporal window determined by the timing signal. The last component is composed of two 4096× eight bit FIFOs and serves as a temporary storage buffer for the data before it is transferred by direct memory access (DMA) to computer memory.

The general sequence of operation for the data acquisition card begins with the detection of the timing signal. The counter is then blocked, preventing any more events from
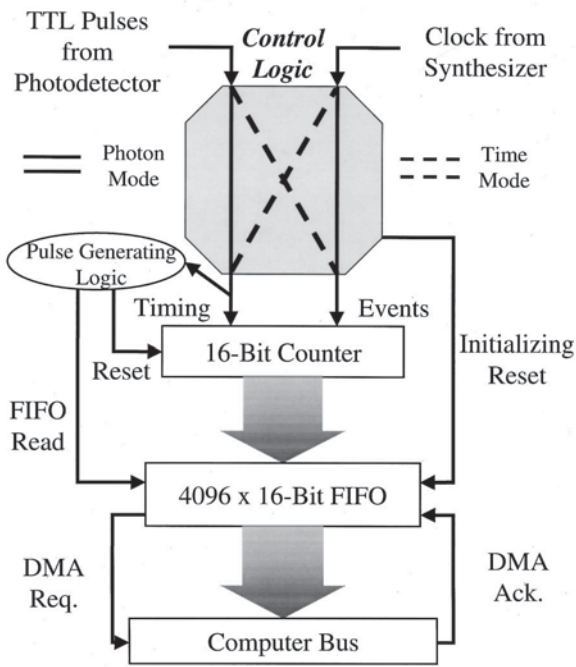
FIG. 3. The overall circuit diagram showing the basic structure of the card. The four units that make up the circuit are the control logic, pulse generating logic, counters, and FIFOs. The event signal causes the counters to count up until a timing signal is received. Then the data is transferred from the counters to the FIFOs and the counters are reset. Switching between the two modes simply swaps which input is the timing signal and which is the event signal.

reaching the counters. A 15 ns pulse is sent to the FIFOs resulting in a FIFO read of the counters' output followed by a 10 ns reset pulse that is sent to the counters. Event signals are once again allowed to reach the counters and the sequence repeats when the next timing signal is detected. This sequence will continue until the number of cycles of data taking desired has been reached. The output of this sequence (in either mode) is the number of rising edges of the event signal that occur in the time span defined by two consecutive rising edges of the timing signal as shown in Fig. 1. The FIFOs temporarily store the output signal until an asynchronous transfer places the output in computer memory using the DMA protocol. The importance of depth for the FIFOs will be discussed later.

The time during which event signals are prevented from reaching the counters is defined as the dead time of the card. In order to minimize the dead time an inverter and several AND gates are used to create the pulses and timing necessary to cause the FIFO read of the counters and then the counter reset. These pulses need to satisfy minimum width requirements as well as occur sequentially. We used two different types of AND gates (F and LS) to customize the timing. Clearly the faster the read and reset can be done, the shorter the dead time. We succeeded in reducing the overall dead time to 25 ns, which is the minimum allowed by the chip components used.

A major consideration in electronic design, especially when wire wrapping, is noise. For this reason the choice of the chip types used is crucial, especially since as a rule of thumb the faster the chip is the greater the noise produced.

So usually one needs to trade off speed in order to reduce noise. Fortunately in going from the ACT type counters to the F counters the speed (max input frequency of 125 MHz) was unaffected while the noise was drastically reduced. Capacitors throughout the board are necessary in order for a wire-wrapped board to function at 60 MHz, and beyond. Low pass filters on the DMA request and acknowledge lines where required since our tri-state FIFOs are directly hooked up to the computer's bus. If those filters are not employed then any noise on those lines could cause the card to hang up, or the computer to crash. Delay logic that prevents the card from making a DMA request too soon after the end of a DMA acknowledge turned out to be necessary in dealing with timing discrepancies between different computer motherboards. Different buses have different timing and noise constraints for the DMA transfer protocol even though the overall structure is standardized.

The DMA single transfer protocol is used to transfer the data from the FIFO to the bus. The empty flag of the FIFO is used as the DMA request signal and the DMA acknowledge pulse from the computer causes the FIFO to write to the bus (i.e., the DMA buffer). Software is then utilized to handle the transfer of data from the DMA buffer to permanent memory (i.e., hard drive, disk, etc.) and ensure that the user is notified if data that has not yet been transferred is overwritten in the DMA buffer. This software is also used to calculate the autocorrelation function and the average counts per second on the fly.

V. TIME MODE

In time mode the event signal is the output from the photon detector, while the timing signal is the output of a frequency generator (i.e., the clock). So the counters on the card will increment every time a signal is received from the detector. When the rising edge of the timing signal is received, the FIFOs read the number that the counters reached and (when the DMA request is acknowledged) write that information to the DMA buffer which is then taken to permanent memory. So the output is a string of numbers, each of which represent the number of photon events between successive rising edges of the clock. Since one cannot know where in the time bin a photon has arrived, the maximum time resolution will be determined by the width of the time bin. Therefore, the greater the clock frequency the higher the temporal resolution. In this mode the data acquisition card requests the bus at the clock frequency. For ISA single mode DMA transfer the maximum theoretical transfer speed is about 0.8 MB/s,[17] which puts a theoretical upper bound on the order of 1 μs, on the time resolution of the time mode. Even if this frequency were attainable (we have found that a clock frequency of about ~0.5 MHz is the practical limit[18] on most computers) this would mean that on average the FIFOs would be transferring zeros, since the photon count rate is an order of magnitude slower. A lot of bandwidth is therefore wasted since the bus transfers 16 bits every time it acknowledges the card's request and yet only the first few of those bits would ever be used.

In order to insure proper operation in this mode the event

signal to the counters is disabled for the duration of the dead time. This is done to prevent the counters' output from changing during the time in which the FIFOs are accessing that output.

VI. PHOTON MODE

This mode was designed to overcome the data transfer inefficiency inherent in the previous transfer protocol. In photon mode the event signal is the clock and the timing signal is the output of the single photon detector. When a photon event is detected, the FIFOs read the output bits of the counters and then the counters are reset. The counters then count up every time the rising edge of a clock is detected until the next photon event. So the output in photon mode is a string of numbers each of which indicate the number of clock cycles between photon events. Again, the higher the frequency of the clock the better one knows the temporal resolution of each photon's arrival. In contrast to the time mode, however, the transfer rate is determined by the frequency of photon events and is independent of the clock frequency.

Although at first glance it may appear that the two modes of operation (time and photon) are entirely symmetric, this is in fact only the case when testing is done with frequency generators. The moment the circuit is actually tested with TTL pulses from a photon detector setup the symmetry is broken because whether or not the timing signal is periodic (time mode) or random (photon mode), matters. The circuitry required for the photon mode is more complex because certain safeguards need to be put in place to handle the random timing signal. One such safeguard involves disabling the timing input line between the time that a stop signal arrives and the time the circuit is once again ready to receive counts (i.e., during the dead time). This is necessary because in this mode it is possible for another timing signal (i.e., photon) to arrive during the dead time of the card. In time mode on the other hand we needed to stop only the event signal's input line. In fact, blocking the timing signal's input line in time mode will result in the creation of extra rising edges due to the 50% duty cycle nature of the output of frequency generators. So the circuit was designed to recognize its mode of operation and block the timing event line only in the photon mode for the duration of its dead time of 25 ns.

Other safeguards revolve around the fact that in the photon mode the circuit needs to be able to handle a large dynamic range in the separation between two consecutive timing signals. This is a result of the uncertainty in the time lapse between any two consecutive photons. In the case of a burst of photons it is important to have a FIFO that has enough depth such that it will not overflow while it waits for the computer to respond to its DMA request. On the other hand, if there is a long time separation between two photons and the frequency of the clock is high then it becomes possible that the counters could overflow. The lower the average rate of photon counts the more likely a scenario this becomes, since the average time between successive photon events increases. A relationship between the probability of

having a counter overflow and the average photon count rate can be derived, assuming that the photon detection process can be modeled as a homogenous Poisson point process.[19] The normalized probability density that two photons are separated by a time t is given by

$$P(t) = ke^{-kt}, \tag{1}$$

where k is the average number of photons detected per second.[20] We define an overflow time, t_{of}, such that successive photons separated by a time greater than t_{of} cause the counters to overflow. To calculate the probability, $P(overflow)$, that the two photons are separated by at least the overflow time, t_{of}, one needs to integrate Eq. (1)

$$P(overflow) = 1 - \int_0^{t_{of}} P(t) dt = e^{-kt_{of}}. \tag{2}$$

The overflow time, t_{of}, depends on the frequency of the clock, f_{clock}, and the number of bits, n, of the counter in the following manner:

$$t_{of} = 2^n / f_{clock}. \tag{3}$$

Equation (2) is the probability of an overflow condition occurring given a single pair of photon events. In order to take into account the total number of photons, M, received in an experiment, we need to modify Eq. (2)

$$P_M(overflow) = 1 - (1 - e^{-kt_{of}})^M. \tag{4}$$

From Eq. (4) we have the probability of a single overflow occurring given M photons, $P_M(overflow)$, as a function of the average number of photons detected, k, for a constant overflow time, t_{of}, determined by the card design. This function transitions from 1 to 0 over a small range of the variable k. The range over which this transition occurs depends on the number of bits, n, the clock frequency, f_{clock}, and the number of photons received, M. So for example, if n, f_{clock}, and M are set to 16 bits, 10 MHz, and ten million photons, respectively, then the range of k in which $P_M(overflow)$ transitions from 0.97 to 0.03 is 2268–2992 cps. As k is increased above 3000 cps the probability of a counter overflow quickly becomes vanishingly small.

As an additional safeguard we disable the counters once their maximum count is reached. This is done to insure that if there is an overflow the counters will not turn over and begin counting from zero again. So the output of the counters would be 2^{16} regardless of the magnitude of an overflow. Due to this design, counter overflows can easily be spotted in our saved data and dealt with as desired. In the interest of future card design the earlier equations can be used to calculate the number of bits, that a counter should possess, such that the probability of an overflow is negligibly small, even for a worst case experimental scenario. In other words for a case in which a high time resolution is required and yet a low flux of photons is available. If we assume a clock frequency, f_{clock}, of 100 MHz, an average number of photons, k, of 200 cps and the detection of ten million photons, M, then the probability of an overflow, $P_M(overflow)$, would be about 3×10^{-8} if the counter had 24 bits.
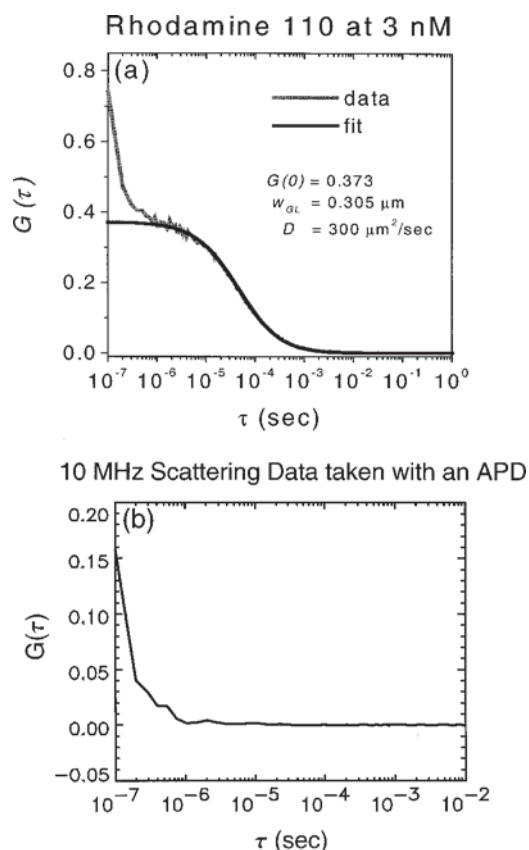
Rhodamine 110 at 3 nM
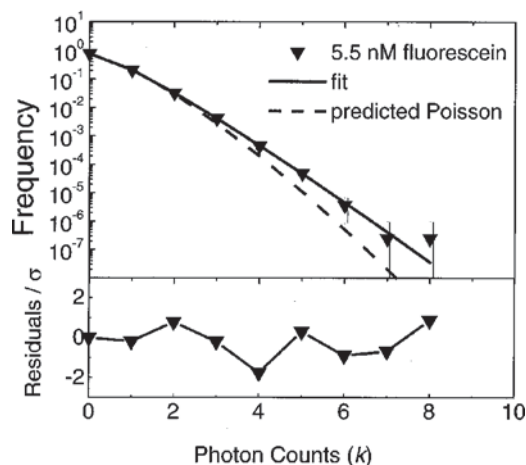

PCH Analysis of Raw Data

FIG. 5. PCH analysis of data obtained from free fluorescein in solution. The deviation from the predicted Poissonian becomes more pronounced towards the tail. The data can be fit using two parameters: the average number of molecules in the excitation volume, N, and the number of counts per second per molecule (i.e., the brightness), ϵ. The residuals of this fit are also shown indicating a good fit of the data. This analysis complements that of the standard autocorrelation because it can separate species based on differences in brightness as opposed to differences in the diffusion coefficient. The emphasis here is on the flexibility in analysis due to the fact that the entire temporal sequence of photon arrivals is stored.

FIG. 4. Photon mode autocorrelation data taken with a 10 MHz clock frequency. (a) Rhodamine data (courtesy of Dr. Yan Chen) depicting APD afterpulsing correlation on the order of 50 ns. The correlation due to the diffusion of Rhodamine through the excitation volume is on the order of 50 μs. The autocorrelation decays to zero indicating no correlation for long time scales. (b) Autocorrelation of scattered laser light data which corroborates the premise that the 50 ns correlation is due to detector afterpulsing and not due to fast kinetics. Without afterpulsing the scatter data would not exhibit any correlation on the time scales measured.

VII. RESULTS

Systematic tests using frequency generators were performed to test our electronic circuit and software design. One of the tests for the photon mode involved a double pulse generator as the photon input and a 9 MHz clock input. The two pulses were separated by 200 ns and repeated every 20 μs. Performing an autocorrelation on the data resulted in three spikes that repeat every 20 μs. The magnitude of the three spikes had a ratio of 1:2:1 reflecting the overlaps of one, both, and then one pulse. The separation between the first and second spike was the same as the separation between the second and third spike, and equal to 200 ns. The photon mode output alternated between two numbers (178 and 2) repeated over and over again. These signified the number of clocks between each pulse arriving from the double pulse generator. In time mode this would have been stretched out to 181 numbers with 178 of them being zeros and the other 3 being ones (representing either the absence or presence of a photon in that bin).

In a subsequent experiment we measured a solution of 3 nM rhodamine using an APD with a time resolution of 100 ns. The data were taken in photon mode and Fig. 4(a) depicts the autocorrelation function that was calculated through soft-

ware. The autocorrelation, $G(\tau)$, decays to zero, indicating that the fluctuations in intensity are independent over long time scales. The correlation time due to the kinetic process of diffusion is seen to be on the time scale of $\sim$50 μs. The fit with a simple translational diffusion model, assuming a 3D-Gaussian for the two-photon excitation volume, is excellent, except for the deviation on the 100 ns time scale due to a very strong correlation. Figure 4(b) demonstrates that this correlation is due to afterpulsing of the APD, since it persists even for a scattered laser light experiment in which the photon counts are not correlated on the time scales accessible by our experimental setup.

In the experiments mentioned earlier we have not utilized the fact that our data acquisition card preserves the entire time resolved sequence of photon arrivals. One major advantage to having all of the data is that it is possible to use analysis other than the autocorrelation function. For example, one can utilize the fact that the histogram of photon arrivals from a fluctuating intensity source is broader then the Poissonian expected of a constant intensity source as can be seen in Fig. 5. For a single species the two parameters that can be used to fit this super-Poissonian curve are the brightness per molecule, ε, and the number of molecules within the observation volume, N.[11] For the general case of m species, $2m$ parameters are required to fit the curve. By using this analysis one can determine the number of species present in the sample.[21,22] In this case ''species'' is defined as a molecule of a specific brightness. Therefore, this method can be used to distinguish between particles that have different brightness but similar diffusion coefficients. In many biological applications, such as the study of dimer formation and dissociation, or enzyme/substrate interactions, the
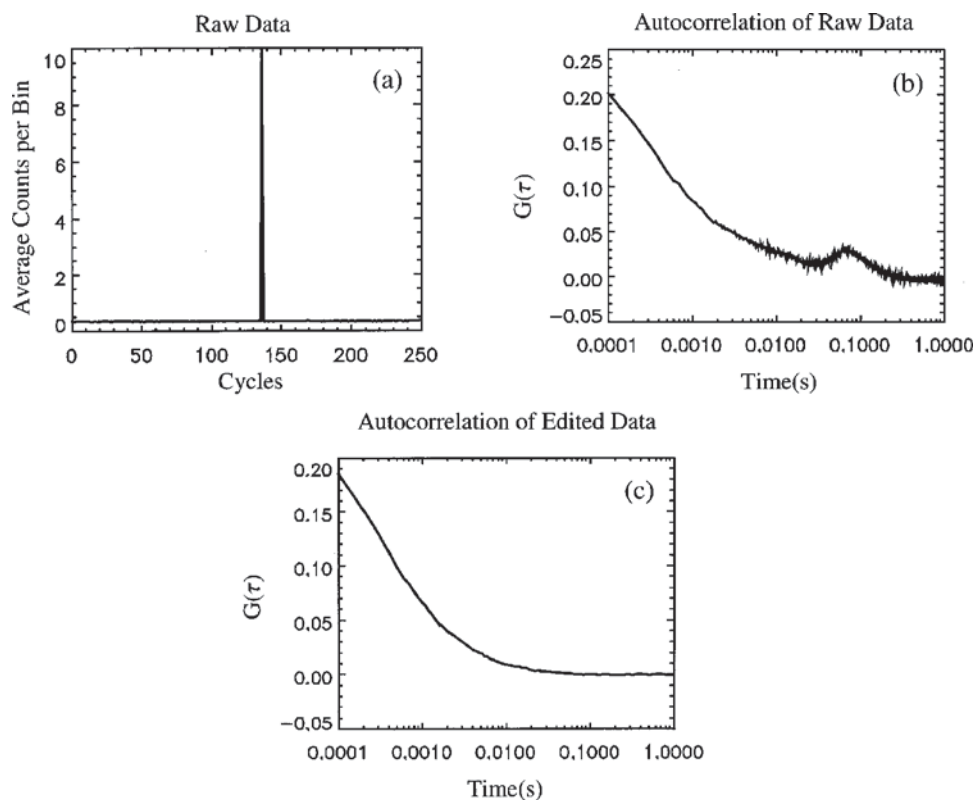
FIG. 6. Time mode data of 20 mer DNA singly labeled with fluorescein taken with a 10 kHz clock frequency. (a) Average counts per bin (0.1 ms) averaged over each DMA buffer transfer cycle (32 Kb) showing an abnormal flux of detected photons in one cycle out of the 250. (b) Autocorrelation of the raw data. (c) Autocorrelation of edited data. The data was edited by removing the cycle in which the abnormal flux of detected photons occurred. This is only possible because the full data set is saved in memory, not just the autocorrelation.

change in the diffusion coefficient is too small to be measured using the autocorrelation function. On the other hand, if the components of the reaction are singly labeled then the brightness will change by a factor of two upon association, and the interaction kinetics can be observed using PCH.

Another advantage resulting from preserving all of the data is that any artifacts present in the original data can be examined and removed if necessary. In Fig. 6(a) an example is shown were a large flux of photons occurs for a short time during the experiment. Figure 6(b) shows that a skewed curve results when the autocorrelation of this data is calculated. The cycle, which represents a full DMA buffer transfer (32 Kb), where the anomalous photon flux occurred can be located and edited out. The resulting autocorrelation, seen in Fig. 6(c), can now be used to calculate a diffusion coefficient. Hardware autocorrelators can only yield the curve shown in Fig. 6(b). This leaves the experimentalist with the unpleasant choice of either retaking the data or attempting to backtrack from the skewed autocorrelation curve by some complex fitting routine with no guarantee of success in either case. In the case where the anomalies themselves may be of interest the task of studying them without interference from the bulk of the data is only feasible if it is possible to directly work with the original data set. One can also imagine running an experiment where the conditions are changed at specific times during the data acquisition process. It is much easier to analyze the different parts of that experiment separately as opposed to trying to make heads or tails of the convolution resulting from the autocorrelation function of the total data set. The earlier examples are by no means an exhaustive list but are intended to give a flavor of the variety of options that are now accessible with this data acquisition card.

VIII. DISCUSSION

Different approaches have been taken over the years to produce faster correlators. The need for correlators sprang up once the field of photon correlation spectroscopy (PCS) began in the 1970's. During that time computers were slow and expensive so the result was the production of no-memory hardware correlators. The hardware design improved from single channel delayed-coincidence measurements, to single stop time-to-amplitude conversion techniques, and then to multistop systems.[10] Nowadays there are excellent multiple-tau hardware correlators available, in terms of resolution and functionality. However, these hardware correlators have two main disadvantages: price and data analysis flexibility. The price is high due to the electronics required to perform the correlations in hardware as well as the need for high temporal resolution. Data analysis flexibility is lost because hardware correlators only return the autocorrelation function and not the raw data.

The incredible increase in computing power has made analysis through software not only feasible, but in most cases more convenient then using highly complex, and therefore expensive, hardware. To analyze the raw data produced by our digital card, we developed software that performs the calculation of the autocorrelation in linear and log time scales as well as in real time. One can therefore use multiple analysis methods on the same data set as well as edit the raw data itself thus giving a more complete picture of the experiment, as was shown in Sec. VII.

Our card reaches the time scale of most hardware correlators and preserves all the information about the temporal distribution of the photons. It also has better dynamic range then commercial hardware correlators since the correlation

can go all the way out to the entire time span of the experiment.

For a given clock frequency the information content of the time and photon modes of our card is, for the most part, equivalent. Deciding which mode to use involves comparing the average number of photons detected per second with the maximum transfer rate of the data acquisition card. One would have to use the time mode if the photon flux rate exceeded the transfer rate of the card (approximately 500 kHz for an ISA card and 10 MHz for a PCI card). To determine which mode has a greater data transfer efficiency one need only compare the frequency of the clock to the average counts per second expected from the sample. The photon mode is more efficient when the average counts per second is less then the clock frequency and vice versa for the time mode. Typically, since we are operating in the single molecule regime for FCS measurements, the average counts per second is less then 100 000. The clock on the other hand is set to as high a frequency as possible due to the need for greater time resolution. In such a scenario, the photon mode is several orders of magnitude more efficient, in terms of data transfer rate, than the time mode.

The design discussed in this article is an ISA data acquisition card. For a PCI version of the card it would be more advantageous to use the PCI bus master transfer protocol which would allow for 32 bit data transfer at a sustainable clock speed of about 10 MHz. One might imagine that with this kind of transfer speed the data transfer efficiency of the photon mode is no longer needed. However, wasting bandwidth is never a good option. The extra speed now available due to advances in computing technology can be used for other things, such as transferring more channels, performing additional real-time calculations on the incoming data, etc. Since the bus transfer is done with either 16 or 32 bits at a time it is inefficient to perform data acquisition in such a way that only the first couple of bits are ever nonzero. In other words, time mode would be a viable option only if it were possible to transfer one or two bits at a proportionally higher rate then it is to transfer 16 or 32 bits. But even if that were possible, the photon mode would still have an advantage because it is a more compact representation of the same information, thus reducing the amount of memory needed to store the data. For a photon rate of 100 kHz, a clock frequency of 10 MHz, and 1000 s of data collection the file will be on the order of 100 Mb for the photon mode and 10 Gb for the time mode.

Ideally one would like to have the counters enabled the entire time because the ultimate limitation on the temporal resolution of this data acquisition card is its finite dead time—the time during which the counters are disabled. This is not possible because some time must be taken, after every timing event is received, to transfer the data to the FIFOs and reset the counters. For our current design, the time during which the counters are disabled is 25 ns. On the other hand, the APDs we used have a dead time of around 30 ns due to their internal quenching circuitry. The PMT we used in our experiments had a dead time on the order of a couple of nanoseconds but its afterpulsing obscures all processes that occur on the microsecond and shorter time scales (data not shown). Therefore, the current limit in time resolution is due to detector effects and not the card's dead time. A scheme involving two entirely independent channels receiving counts from two independent detectors has been used to get around these limitations.[23] This design consists of continually alternating between the two independent channels either through hardware or software. In this manner, first order effects due to afterpulsing and dead times would be eliminated since neither of those effects would correlate across the independent channels. This design would require the use of a beam splitter to separate the signal onto the two detectors, thus resulting in the loss of half of the photon counts. Higher order dead time effects will still be present since it is possible to have more photon events during the dead time, then independent channels. But these effects would, for the most part, be negligible. It is worthy to note that the general structure of our single channel data acquisition board is such that it can easily be scaled to multichannel capability. So, in order to construct a multichannel version one simply needs to place multiple copies of the current version on the same board, in addition to some very simple logic that continually switched between the channels after each photon is received. This is of great interest because a multichannel version of this board will allow for the use of such techniques as fluorescence resonance energy transfer and cross correlation.

IX. CURRENT DEVELOPMENTS

In collaboration with ISS (Champaign, IL) a dual channel, 32 bit, PCI version of our design has been implemented. Unlike the switching scheme proposed earlier, this card saves all of the data from both channels. In this way one can do the switching through software at some later time, to nullify dead time and detector artifacts, or analyze each of the channels independently, since none of the photons are lost. The cost of using this method is that it transfers data at half the speed and takes up twice as much memory as the hardware switching scheme mentioned earlier.

In addition to a multichannel version of the data acquisition card, other functions can be developed that would provide additional information. The raw data, from either mode of operation, gives information about the temporal separation between photon arrivals but does not yield the time lapse between laser excitation and fluorescence emission—the lifetime. Combining this extra dimension to the available FCS analysis yields a very powerful observational technique.[24] To address this issue we have designed additional circuitry that is used to measure the lifetime of the detected fluorescence. In conjunction with a multichannel version of the card this addition will allow us to obtain multiple order autocorrelation functions, PCH, cross-correlation function, and lifetime information from a single experimental data set.

ACKNOWLEDGMENTS

[1] D. Magde, E. Elson, and W. W. Webb, Phys. Rev. Lett. **29**, 705 (1972).

[2] M. Ehrenberg and R. Rigler, Chem. Phys. **4**, 390 (1974).

[3] S. R. Aragon and R. Pecora, J. Chem. Phys. **64**, 1791 (1976).

[4] J. Widengren, R. Rigler, and U. Mets, J. Fluoresc. **4**, 255 (1994).

[5] E. L. Elson and D. Magde, Biopolymers **13**, 1 (1974).

[6] D. Magde, E. L. Elson, and W. W. Webb, Biopolymers **13**, 29 (1974).

[7] D. Magde, Q. Rev. Biophys. **9**, 35 (1976).

[8] G. Feher and M. Weissman, Proc. Natl. Acad. Sci. USA **70**, 870 (1973).

[9] R. D. Icenogle and E. L. Elson, Biopolymers **22**, 1919 (1983).

[10] C. J. Oliver, in *Photon Correlation and Light Beating Spectroscopy*, edited by H. Z. Cummins and E. R. Pike (Plenum, New York, 1973), Vol. 3, p. 75.

[11] Y. Chen *et al.*, Biophys. J. **77**, 553 (1999).

[12] A. G. Palmer III and N. L. Thompson, Biophys. J. **52**, 257 (1987).

[13] A. G. d Palmer and N. L. Thompson, Chem. Phys. Lipids **50**, 253 (1989).

[14] H. Qian and E. L. Elson, Biophys. J. **57**, 375 (1990).

[15] K. M. Berland, P. T. C. So, and E. Gratton, Biophys. J. **68**, 694 (1995).

[16] A. Ellington, in *Current Protocols in Molecular Biology* (Wiley, New York, 1993).

[17] T. Shanley and D. Anderson, *ISA System Architecture*, 2nd ed. (Mind-Share, Inc., Richardson, TX, 1991).

[18] For each individual computer the maximum practical card transfer speed in time mode can be experimentally verified by noting the frequency of the clock at which the DMA acknowledge signal just begins to overlap with the DMA request signal.

[19] Strictly speaking the photon detection process is a doubly stochastic Poisson point process (see Ref. 20), but it is well approximated by a homogenous Poisson point process for the relatively long time scales of interest here.

[20] B. Saleh, *Photoelectron Statistics, with Applications to Spectroscopy and Optical Communications* (Springer, Berlin, 1978).

[21] J. D. Müller *et al.*, Biophys. J. **76**, A359 (1999).

[22] J. D. Müller, Y. Chen, and E. Gratton, Biophys. J. (in press).

[23] M. A. Finn, G. W. Greenlees, and T. W. Hodapp, Rev. Sci. Instrum. **59**, 2457 (1988).

[24] C. Eggeling *et al.*, Proc. Natl. Acad. Sci. USA **95**, 1556 (1998).